Dalton Transactions

ROYAL SOCIETY OF CHEMISTRY

PAPER

View Article Online
View Journal | View Issue

Cite this: *Dalton Trans.*, 2025, **54**, 1972

Synthesis, characterization and functionalization of titanium κ^1N amidinato complexes from carbodiimides†

Marcel Eilers, Saskia Bültena, Kevin Schwitalla, Marc Schmidtmann and Rüdiger Beckhaus *

Received 21st November 2024,
Accepted 9th December 2024

DOI: 10.1039/d4dt03261f

rsc.li/dalton

A series of titanium amidinato complexes were synthesized by stoichiometric insertion reactions of carbodiimides into bis(π–η^5:σ–η^1-pentafulvene)titanium complexes. NMR studies and single-crystal X-ray diffraction showed κ^1N coordination of the former carbodiimides to the metal center. DFT calculations were performed, confirming the clear preference for a single nitrogen atom coordinating to the metal center with a high energy transition state for the formation of a chelating heteroallyl ligand. Depending on the pentafulvene ligand, additional insertion reactions of carbodiimides into the remaining Ti–C_{exo} bond were observed. This allows for a stepwise insertion of the corresponding carbodiimides and offers the possibility to further functionalize the complexes. The reactivity of the remaining pentafulvene ligand is further demonstrated in reactions with H-acidic and multiple bond substrates.

Introduction

Carbodiimides (**I**) are prominent members of the large family of cumulenes, starting with allene (**II**) itself and the heterocumulenes (**III**), like carbon dioxide, isocyanates or isothiocyanates (Fig. 1).

Due to the broad variability of the substitution patterns, carbodiimides (**I**) are important building blocks with many different organic and catalytic processes relying on this reactive class. They are widely used in organic synthesis and probably best known for their catalytic use in the synthesis of peptides, amides, and esters,[1] for example in the total synthesis of penicillin discovered by Sheehan and co-workers.[2] They may also be used in hydroboration reactions[3] or in guanylation reactions leading to the formation of guanidine-based ligands.[4] Only a few carbodiimide-based metal complexes have been synthesized, such as carbodiimido titanium complexes by salt metathesis reactions (Fig. 2a).[5] The central carbon atom of the carbodiimides is positively polarized and can therefore be attacked by nucleophiles. This led to the insertion of several carbodiimides into various metal–element bonds, for example M–C, M–O, M–B and M–N bonds, resulting in the formation of chelating heteroallyl complexes (Fig. 2b).[6] Some of these titanium complexes have been shown to be useful in catalytic living polymerisation reactions by exploiting the insertion reaction.[7] Remarkable results were achieved by the groups of Rosenthal and Tonks with unusual four-membered heterometallacarbene complexes by replacing the alkyne in the Cp_2Ti (btmsa) complex with various carbodiimides (Fig. 2c).[8]

On the other hand, examples for 1,2-insertion reactions of the carbodiimide into M–C bonds (Fig. 2d),[9] and (reversible) cycloaddition reactions[10] with M=N complexes were reported. For many years, our group has been pursuing the fundamental chemistry and synthetic applications of bis(π–η^5:σ–η^1-pentafulvene)complexes of group 4 and 5 transition metals. These have been shown to be excellent precursors for the functionalization of transition metal complexes by either E–H bond activation[11] or multiple bond substrate insertion[11k,l,12] into the frustrated M–C_{exo} bond in almost always salt free reactions under mild conditions and in high yields. Within our studies, we recently reported on the insertion reaction of carbodiimides into a vanadium pentafulvene complex, forming a vanadium κ^1N amidinato complex.[11l] This led to further investigations into reactions of pentafulvene complexes with cumulated sub-

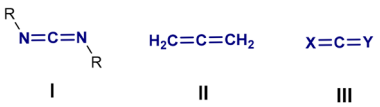

Fig. 1 Carbodiimides (I), propa-1,2-diene (II) and hetero-cumulenes (III).

Institut für Chemie, Carl von Ossietzky Universität Oldenburg, D-26111 Oldenburg, Germany. E-mail: ruediger.beckhaus@uol.de

†Electronic supplementary information (ESI) available. CCDC 2402660–2402670 and 2404156. For ESI and crystallographic data in CIF or other electronic format see DOI: https://doi.org/10.1039/d4dt03261f

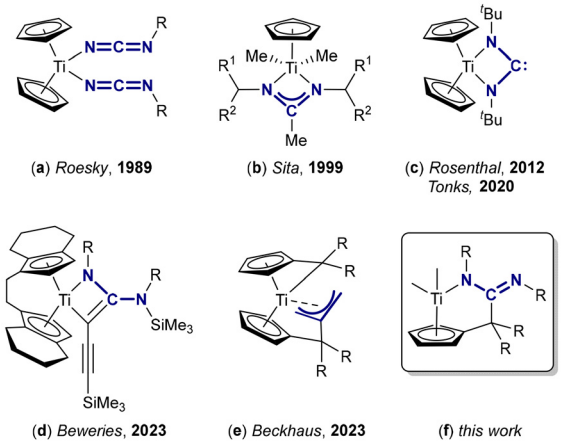

Fig. 2 Selected examples of titanium–carbodiimide complex (a), carbodiimides inserted into M–C bonds (b), recent example of carbodiimide coordination (c) and 1,2-insertion (d), along with an example for an allyl complex derived from the reaction of **1** with propa-1,2-diene (e) and this works 1,2-insertions of carbodiimides (f).

strates and the recently published reaction of the bis(π–η^5:σ–η^1-pentafulvene)titanium complex **1** with propa-1,2-diene and the formation of chained titanium–allyl complexes (Fig. 2e).[13] Continuing our recent investigations, we herein report on the reaction of bis(π–η^5:σ–η^1-pentafulvene)titanium complexes with either one or two equivalents of carbodiimides. We further demonstrate the reactivity of the obtained titanium κ^1*N* amidinato complexes (Fig. 2f) towards E–H activation and multiple bond substrate insertion.

Results and discussion

Synthesis and characterization of insertion products

We investigated the stoichiometric reactions of **1** with symmetrical carbodiimides RN=C=NR (R = ^{i}Pr, Cy, ^{t}Bu, SiMe$_3$, Dipp; Dipp = 2,6-diisopropylphenyl) at room temperature. The more sterically challenging derivatives (^{t}Bu, SiMe$_3$ and Dipp) showed no reaction even at elevated temperatures (80 °C). This could have been due to the steric hindrance and the importance of the precoordination of a nitrogen atom of the carbodiimide to the metal center. Gambarotta and co-workers already studied the mechanism of insertions of carbodiimides and other heterocumulenes into zirconium–alkyl bonds and proposed the coordination as the first step in insertion reactions for carbodiimides.[6i] The resulting polarization of the N=C=N fragment led to the migration of the alkyl group to the central carbon atom of the former carbodiimide. The same outcome was found by Tunge, who mentioned the importance of the dissociation of THF to allow coordination of carbodiimides to the metal center.[6j]

With less sterically demanding substituents, the reaction of **1** with iso-propyl and cyclohexyl carbodiimides at room temperature resulted in an immediate colour change of the solutions from blue (**1a**) and green (**1b**) to red (**2** and **3**). The colour change can be explained by the prior coordination of one nitrogen atom of the carbodiimide to the metal center. By following the reaction with ^{1}H NMR spectroscopy, an additional set of signals for the adduct formation was observed (see ESI, Fig. S3†). The characteristic ^{i}Pr–H signals for the carbodiimide adduct are found at δ^1H = 3.65 and 3.94 ppm and are low field shifted compared to the free ^{i}PrN=C=N^{i}Pr (δ^1H = 3.33 ppm) and to the product signals of **2a** (δ^1H = 3.10 and 3.25 ppm).

Coordination of strong donors to bis(π–η^5:σ–η^1-pentafulvene)titanium complexes has been previously observed by our group in reactions with NHCs,[14] and the formation of a Lewis acid–base complex between CyN=C=NCy and PhBCl$_2$ as an intermediate in the insertion reaction of carbodiimides into a boron–aryl bond was found by Cowley and co-workers.[15] The prior coordination of carbodiimides to titanium centers has only been found in theoretical studies.[16]

After stirring the red solutions for several hours, the formation of green precipitates was observed. The supernatant was decanted and the solids washed with a small amount of *n*-hexane and dried in high vacuum. The obtained green solids were isolated in moderate (**3b**: 52%) to very good yields (**2a**: 93%, **2b**: 80%, **3a**: 80%) at the gram scale. They are air and moisture sensitive and were therefore stored in a glovebox (Scheme 1).

The products were characterized by NMR spectroscopy and the coordination mode was determined by single-crystal X-ray diffraction (SC-XRD). In accordance with the asymmetric chemical environment at the titanium center, in the ^{1}H NMR spectra the eight characteristic signals for the eight independent cyclopentadienyl (Cp) protons are found in the range of δ^1H = 3.96–6.79 ppm (**2**) and δ^1H = 3.41–6.17 ppm (**3**). The signals for the protons of the respective carbodiimides are observed at higher fields, next to the signals for the adamantyl (CH/CH$_2$) and *para*-tolyl (CH$_3$) protons. For **2**, one adamantyl signal gets significantly shifted to lower fields (δ^1H = 4.17–4.26 ppm), probably due to hydrogen bridging to the imine nitrogen atom of the former carbodiimide. The ^{13}C{^{1}H} chemical shifts of the former quaternary carbon atoms of the carbodiimides are found at δ^{13}C{^{1}H} = 173.1 (**2a**), 172.5 (**2b**), 175.2 (**3a**) and 175.1 (**3b**) ppm, which are significantly shifted to lower fields compared to the free carbodiimides (*cf.* R^1 = Cy: 139.8 ppm).[17] For **3a**, the ^{15}N signals, obtained from a ^{1}H,^{15}N-HMBC spectrum, show values of δ^{15}N = 276.7 and 278.2 ppm for the nitrogen atoms by coupling with the respect-

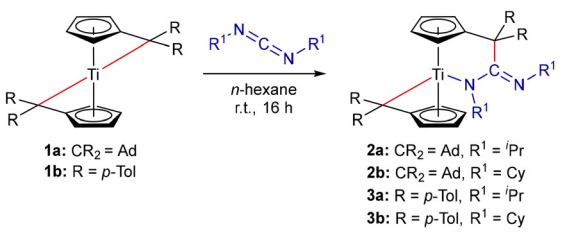

Scheme 1 Insertion reactions of **1** with symmetrical carbodiimides to form titanium κ^1*N* amidinato complexes **2** and **3**.

ive iso-propyl protons. A second set of signals can be observed in the NMR spectra of **2b**. A characteristic shift of $\delta^{13}C\{^1H\}$ = 160.1 ppm for the central carbon atom of the former carbodiimide indicates the migration of a cyclohexyl group from one nitrogen to the other and the formation of an η^1-imino complex **2b′** as a side-product (see ESI, Fig. S6†). The chemical shift is between the free carbodiimide (R = Cy: 139.8 ppm)[17] and the insertion product **2b** $\delta^{13}C\{^1H\}$ = 172.5 ppm and would match with literature ($\delta^{13}C\{^1H\}$ = 157.9 ppm).[9] However, a more precise characterization was difficult due to the absence of single-crystals, poor solubility in common solvents such as benzene, toluene, THF, DCM or chloroform and signal overlap.

The formation of the titanium κ^1N amidinato complexes **2** and **3** was also determined by SC-XRD. Suitable crystals were obtained either directly out of the reaction mixtures or by slow evaporation of concentrated benzene-d_6 or *n*-hexane solutions. The solid-state structures of **2a** and **3a** are shown in Fig. 3, the structures of **2b** and **3b** can be found in the ESI.†

The molecular structures of **2** and **3** confirm the insertion of the carbodiimides into one of the two Ti–C_{exo} bonds. With a slightly shortened, when compared to the sum of covalent radii ($\sum r_{cov}$(Ti–N) = 2.07 Å),[18] Ti–N single bond (**2a:** 2.0292(15) Å, **2b:** 2.0466(18) Å, **3a:** 2.0499(5) Å, **3b:** 2.0595(17) Å), the complexes are in accordance with a complex from Beweries and coworkers ((Ti–N) = 2.0562(9) Å).[9] The former Cp–C_{exo} bonds (*cf.* **1b:** 1.453(3) Å),[19] are elongated to approximately 1.52 Å (**2a:** 1.517(2) Å, **2b:** 1.523(3) Å, **3a:** 1.5187(8) Å, **3b:** 1.521(3) Å) due to the change in hybridization of the carbon atom. The newly formed C_{exo}–CN bonds (**2a:** 1.556(3) Å, **2b:** 1.538(3) Å, **3a:** 1.5643(7) Å, **3b:** 1.567(3) Å) are elongated C(sp^3)–C(sp^2) single bonds (1.51)[20] with the former central carbon atom of the carbodiimides being sp^2 hybridized. The remaining Ti–C_{exo} bond lengths (**2a:** 2.446(2) Å, **2b:** 2.469(2) Å, **3a:** 2.4634(6) Å, **3b:** 2.469(2) Å) are only slightly elongated compared to the starting material (**1b** 2.408(2) Å/2.392(2) Å). Overall, complexes **2** and **3** differ only slightly in bond lengths.

We calculated the free Gibbs energies of **2a** and the possible chelating coordination mode of the inserted carbodiimide and found a high transition state of 141.6 kJ mol^{-1} for the exchange reaction between the two nitrogen atoms. The mechanism seems to be associative due to the formation of a hetero-allyl-type transition state, but at the same time, the Ti–C_{exo} bond gets significantly elongated and the Cp–C_{exo} bond retained to the plane of the Cp ring, indicating an ambiguous mechanism with a transition of the σ–η^5:π–η^1 coordination mode to η^4 (see Fig. 4). In contrast to previously reported insertion products and our previously synthesized titanium allyl complex,[13] the coordination of only one nitrogen to the titanium center is the thermodynamic minimum, while the heteroallyl coordination was found to be the transition state of the exchange reaction.

Of the starting complexes **1a** and **1b**, only **1b** reacted with an additional equivalent of carbodiimide, despite the absence of significant differences in Ti–C_{exo} bond lengths. After 16 hours of stirring, the reaction mixtures turned from green to yellow to purple. After workup, the obtained complexes **4a** (78%) and **4b** (58%) were isolated as purple solids (Scheme 2).

The formation of the titanium bis(κ^1N-amidinato) complexes **4a** and **4b** was observed in solution by NMR spectroscopy. The ^1H NMR spectra revealed the symmetrical structure by giving only four characteristic signals in sets of two for the Cp protons. Additionally, the complete set of signals is reduced by a factor of two, which demonstrates the high symmetry of the complexes. In the $^{13}C\{^1H\}$ NMR spectra, only one signal can be observed for the carbon atoms of the former carbodiimides (**4a:** $\delta^{13}C\{^1H\}$ = 173.8 ppm, **4b:** $\delta^{13}C\{^1H\}$ = 175.3 ppm), and for **4a**, the ^{15}N values were found to be $\delta^{15}N$ = 260.9 and 267.5 ppm. SC-XRD of crystals obtained from satu-

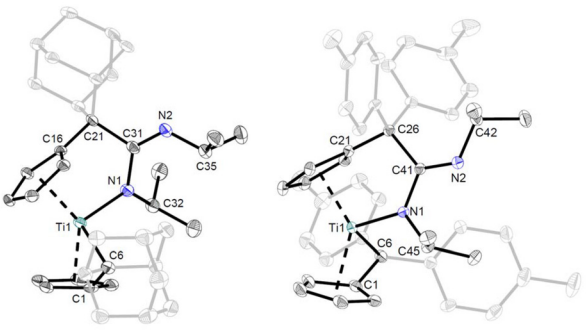

Fig. 3 Molecular structures of complex **2a** and **3a**. Thermal ellipsoids drawn at the 50% probability level. Hydrogen atoms and solvent molecules are omitted for clarity.

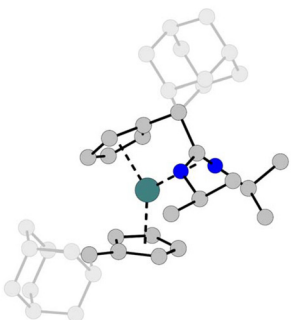

Fig. 4 Calculated structure of the transition state. DFT calculations in toluene (B3LYP/Def2-TZVP).

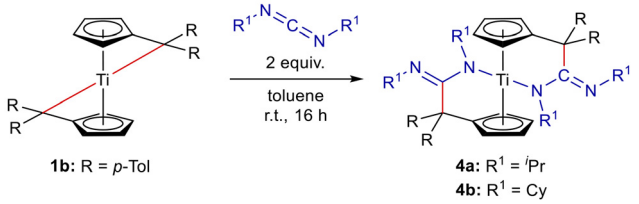

1b: R = *p*-Tol

4a: R^1 = ^{i}Pr
4b: R^1 = Cy

Scheme 2 Reaction of **1b** with two equivalents of carbodiimides to form bis(κ^1N-amidinato) products **4a** and **4b**.

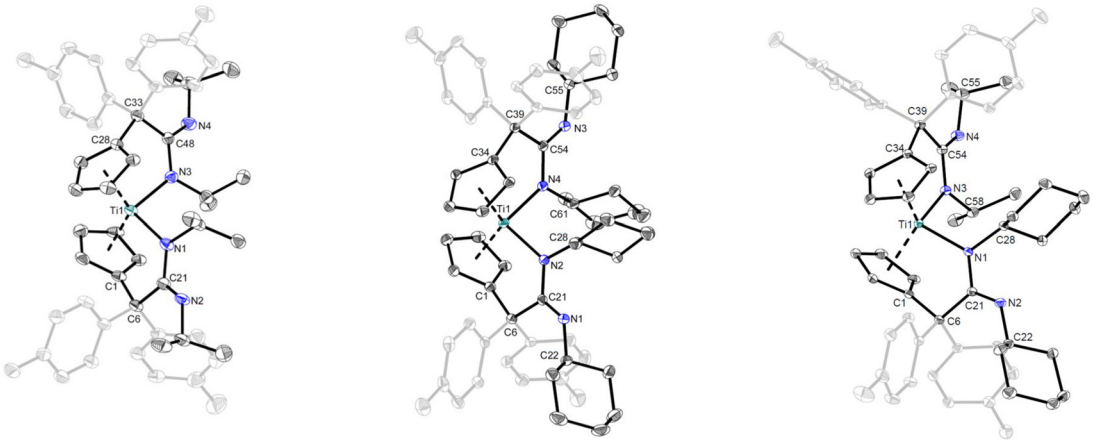

Fig. 5 Molecular structures of complexes **4a** (left), **4b** (middle) and **4c** (right). Thermal ellipsoids drawn at the 50% probability level. Hydrogen atoms and solvent molecules are omitted for clarity.

rated benzene-d_6 solutions by slow evaporation confirms these findings. The molecular structures of **4a** and **4b** are shown in Fig. 5, the structural parameters can be found in the ESI.†

The molecular structures of **4a** and **4b** confirm the double insertion of the carbodiimides into the two Ti–C_{exo} bonds with two Ti–N single bonds (**4a**: 2.055(3) Å, 2.058(3) Å; **4b**: 2.0659 (11) Å, 2.0742(12) Å). Now both former Cp–C_{exo} bonds are elongated due to the insertion and change in hybridization of the carbon atom (**4a**: 1.524(5) Å, 1.523(4) Å; **4b**: 1.5170(19) Å, 1.5131(19) Å). The newly formed C_{exo}–CN bonds (**4a**: 1.557(4) Å, 1.564(4) Å; **4b**: 1.5642(18) Å, 1.5655(18) Å) are also elongated $C(sp^3)$–$C(sp^2)$ bonds.

We were also able to carry out a stepwise double insertion reaction by using *n*-hexane as the solvent in the first step and reacting the isolated complexes **3** with another carbodiimide to obtain the asymmetric complex **4c**, which was carried out on the NMR scale. The formation of the mixed complex **4c** was observed in both cases (Scheme 3).

The ^{1}H NMR spectrum of **4c** shows the asymmetry of the structure by giving eight characteristic signals for the eight Cp protons. Both sets of signals for the cyclohexyl and the isopropyl protons can be observed, and the $^{13}C\{^1H\}$ NMR spectrum shows two signals for the central carbon atom of the former carbodiimides ($\delta^{13}C\{^1H\}$ = 174.3 ppm (NCN–Cy), $\delta^{13}C\{^1H\}$ = 174.5 ppm (NCN–^{i}Pr)). Notably, these double insertion reactions were not observed in reactions of **1** with propa-1,2-diene.[13] The solid-state structure of **4c** is also shown in Fig. 5.

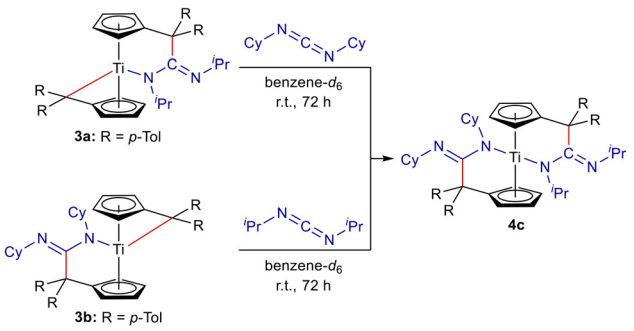

Scheme 3 Reaction of **3** with different carbodiimides to form the asymmetric bis(κ^1*N*-amidinato) complex **4c**.

Reactivity of 2a towards H-acidic substrates

Since **2a** showed no reaction with an additional equivalent of carbodiimide, we were interested in the reactivity of the remaining fulvene ligand. Therefore, we tested H-acidic and other multiple bond substrates in addition to the carbodiimides. We began to investigate the reactivity with various alcohols and amines. Unfortunately, the reaction of **2a** with alcohols (MeOH, EtOH, ^{t}BuPhOH) gave only mixtures of uncharacterized products, indicating a reactivity towards H-acidic substrates but leading to unselective reactions. However, the reaction of **2a** with primary aromatic amines in *n*-hexane (*para*-toluidine) and toluene (2,6-xylidine) at room temperature resulted in a colour change of the reaction mixtures from green (**2a**) to red (**5a**) and orange (**5b**). Solution NMR spectra of the isolated solids revealed selective protonation of the remaining exocyclic carbon atom of the Cp ring (Cp–C_{exo}), resulting in the formation of titanium amido complexes **5** (Scheme 4, top).

Characteristic singlets for the Cp–C_{exo}H protons are found at δ^1H = 2.80 ppm (**5a**) and δ^1H = 2.75 ppm (**5b**) with the corresponding N–H signals at δ^1H = 8.38 ppm (**5a**) and δ^1H = 7.87 ppm (**5b**). The quaternary carbon atoms of the former carbodiimide are found at $\delta^{13}C\{^1H\}$ = 163.8 ppm (**5a**) and at $\delta^{13}C\{^1H\}$ = 165.2 ppm (**5a**), and in the IR spectra, the corresponding N–H frequencies are found at 3363 cm^{-1} (**5a**) and 3325 cm^{-1} (**5b**). In addition, single crystals of **5a** were obtained from a saturated benzene-d_6 solution in the NMR-tube, that were suitable for SC-XRD and confirmed the proposed protonation of the C_{exo} carbon atom. The molecular structure of **5a** is shown in Fig. 6, and the structure of **5b** is given in the ESI.†

The obtained molecular structure of **5a** confirms the protonation of the C_{exo} with an elongated C1–C6 bond to 1.5168(19)

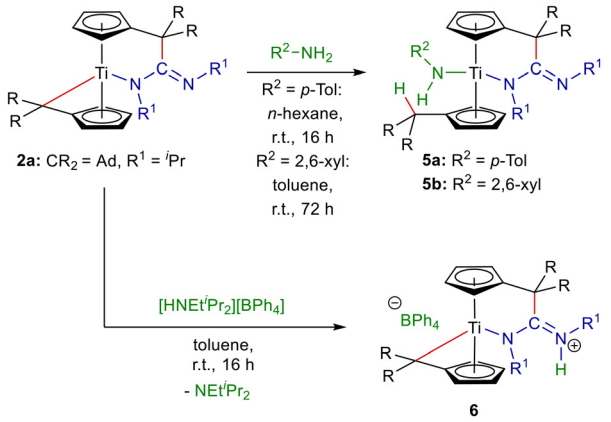

Scheme 4 Reaction of **2a** with primary aromatic amines to give **5** and with an ammonium borate to give **6**.

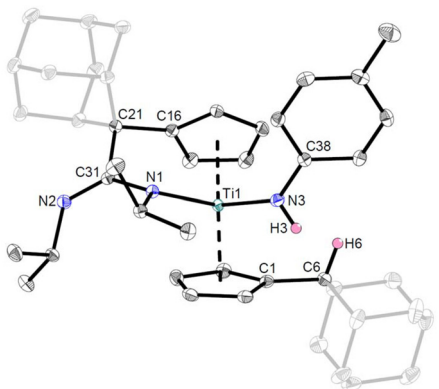

Fig. 6 Molecular structure of complex **5a**. Thermal ellipsoids drawn at the 50% probability level. Hydrogen atoms (except for H3 and H6) are omitted for clarity.

Å and a newly formed Ti1–N3 single bond (1.9872(13) Å), which is relatively short in comparison to the sum of the covalent radii, while the Ti1–N1 single bond has been elongated from 2.031(3) Å to 2.0741(12) Å in the process.

Interestingly, the reaction of **2a** with the ammonium borate $[Et_2NH^iPr][BPh_4]$, did not lead to the protonation of the C_{exo} carbon atom of the pentafulvene ligand, but instead to the protonation of the C=N nitrogen atom of the former carbodiimide (Scheme 4, bottom). This protonation could be an indication of the non-selective reactions of **2a** with alcohols and much stronger acids such as etheric HCl or HOTf, because both the fulvene function and the former carbodiimide can be involved in the reaction. Unfortunately, no single crystals of **6** could be obtained due to the low stability of the cationic complex in solution, as it decomposes in solvents such as THF, DCM and $CDCl_3$ within a few hours. In the solid state, the complex is much more stable and can be stored in a glovebox without decomposing. The protonation of the nitrogen atom was detected in the solution NMR spectra. In the ^{1}H NMR spectrum, a broad doublet is found at δ^1H = 6.73 ppm with a coupling constant of ^3J = 10.0 Hz. This signal is coupling to one of the ^{i}Pr-CH protons, resulting in a doublet (^3J = 10.0 Hz) of a septet (^3J = 6.3 Hz). In the $^{13}C\{^1H\}$ NMR, the quaternary carbon of the former carbodiimide is shifted to $\delta^{13}C\{^1H\}$ = 172.5 ppm and in the $^{11}B\{^1H\}$ NMR, only one signal can be observed at $\delta^{11}B\{^1H\}$ = −6.6 ppm. The characteristic ν(N–H) band can also be observed in the IR spectrum at 3391 cm^{-1}.

Reactivity of 2a towards multiple bond substrates

Given that **2a** reacts with H-acidic substrates, we were interested in its reactivity towards multiple bond substrates other than carbodiimides. Indeed, the reaction of **2a** with acetone in *n*-hexane at room temperature resulted in a colour change of the suspension from green to yellow and the formation of a yellow precipitate. After decanting the supernatant and washing the residue with a small amount of *n*-hexane, the insertion product **7** was isolated in a moderate yield of 40% as a pale yellow solid (Scheme 5, top).

In the ^{1}H NMR spectra, two singlets for the methyl groups of the inserted acetone are observed at δ^1H = 1.21 and 1.41 ppm. In the $^{13}C\{^1H\}$ NMR spectra, the chemical shift for the quaternary carbon atom of the former acetone is shifted to $\delta^{13}C\{^1H\}$ = 110.0 ppm. The ^{15}N chemical shifts of the two nitrogen atoms were found at δ^{15}N = 240.6 and 260.9 ppm. Single crystals were obtained from a saturated solution of benzene-d_6 by slow evaporation and SC-XRD analysis provided the molecular structure confirming the formation of **7** (Fig. 7).

The insertion of acetone leads to the formation of a highly elongated C28–C38 bond of 1.6284(12) Å and the elongation of the former Cp–C_{exo} bond to 1.5211(12) Å. The resulting Ti1–O1 bond length of 1.8689(7) Å is in the range of a shortened single bond when compared to the sum of the covalent radii ($\sum r_{cov}$(Ti–O) = 1.99 Å).[18] The Ti1–N1 single bond has been

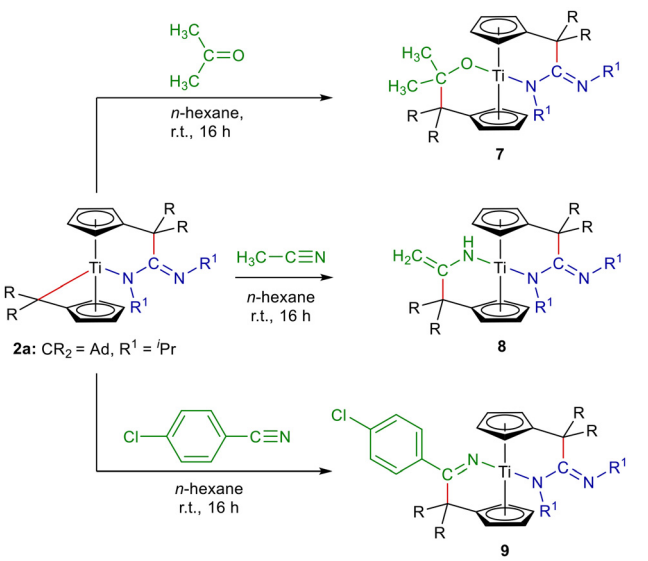

Scheme 5 Functionalization of **2a** with acetone, acetonitrile and 4-chlorobenzonitrile to give **7–9**.

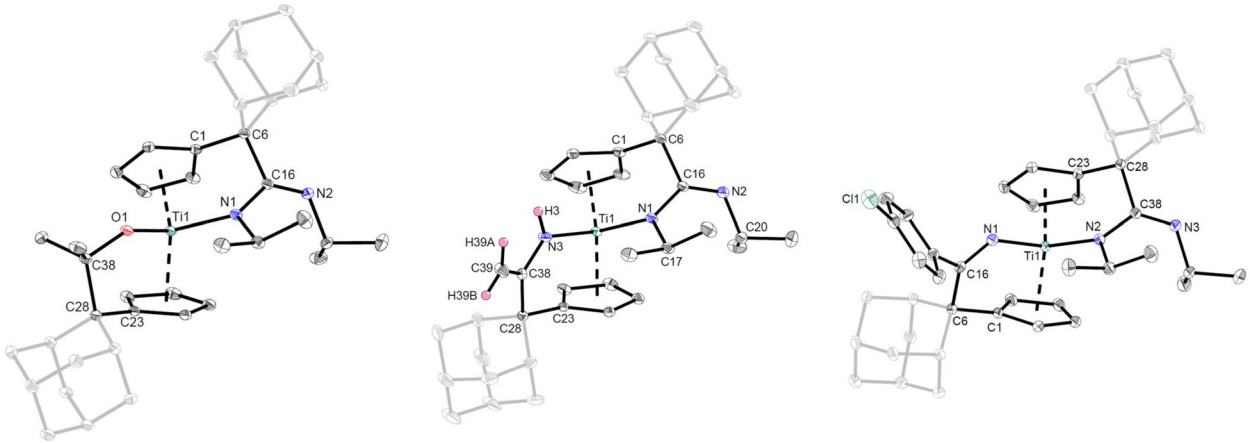

Fig. 7 Molecular structures of complexes **7** (left), **8** (middle) and **9** (right). Thermal ellipsoids drawn at the 50% probability level. Hydrogen atoms (except for **8**: H3, H39A, H39B) and co-crystallized solvent molecules for **9** are omitted for clarity.

slightly elongated from 2.031(3) Å to 2.0528(8) Å in the process.

We were also able to react **2a** with acetonitrile and 4-chlorobenzonitrile, which also inserted into the remaining Ti–C_{exo} bond, while the product of the reaction with acetonitrile additionally underwent a 1,3-H-shift to form the amido complex **8** (Scheme 5, middle). This shift cannot be observed on the NMR timescale, leading to the isolation of the amido complex **8** in 77% yield. In the ^{1}H NMR spectrum, the characteristic singlets for the two terminal alkene protons are found at δ^1H = 3.77 ppm and 4.30 ppm. This is in accordance with the absence of the former methyl group of acetonitrile. The proton of the formed amido ligand is observed as a broad singlet at δ^1H = 7.35 ppm. The corresponding ^{15}N cores were observed at δ^{15}N = 232.8 (NCN), 258.5 (NCN) and 262.5 (NH) ppm. In the IR spectrum, the characteristic ν(N–H) band is found at 3351 cm^{-1}.

We were also able to obtain the molecular structure through SC-XRD from single crystals of a saturated benzene-d_6 solution. The molecular structure of **8** is shown in Fig. 7. The insertion of acetonitrile and the following 1,3-H-shift resulted in the formation of a new elongated C28–C38 single bond (1.5429(13) Å). The 1,3-H-shift is seen in the C38–C39 double bond (1.3505(13) Å), which is now a slightly elongated C(sp^2)=C(sp^2) bond (1.32 Å).[20] The resulting new Ti1–N3 bond with 1.9768(8) Å is in the range of a shortened single bond, and the Ti1–N1 single bond has been slightly elongated from 2.031(3) Å to 2.0562(8) Å in the process.

To negotiate this 1,3-H-shift, we used 4-chlorobenzonitrile and observed a colour change from green to pink and a pink precipitate formed, which was isolated by decantation of the supernatant and washing of the residue with a small amount of *n*-hexane to result in an 80% yield (Scheme 5, bottom). The aromatic protons are found in the ^{1}H NMR spectrum at δ^1H = 6.61–7.11 ppm. Additionally, crystals suitable for SC-XRD analysis were obtained from a saturated benzene-d_6 solution by slow evaporation of the solvent. The molecular structure is shown in Fig. 7. The insertion of 4-chlorobenzonitrile resulted in the formation of a new elongated C6–C16 single bond (1.5695(14) Å). With 1.2709(13) Å, the former triple bond of the nitrile now lies in the range of a shortened C(sp^2)=N double bond (1.28 Å).[20] The resulting new Ti1–N1 bond is 1.9861(9) Å, which is in the range of a shortened single bond. The Ti1–N2 single bond has been slightly elongated from 2.031(3) Å to 2.0461(9) Å in the process.

Conclusions

In this work, we performed reactions of bis(π–η^5:σ–η^1-pentafulvene)titanium complexes with carbodiimides under mild conditions. Selective insertions of the carbodiimides into the Ti–C_{exo} bond were observed. These insertion reactions led to the κ^1*N* coordination of one nitrogen atom to the titanium center with no indication for the heteroallyl coordination mode. This was further supported by DFT calculations, showing a heteroallyl-like transition state at relatively high energy and demonstrating the electronical flexibility of the pentafulvene complexes. The reactivity of the isolated complexes was investigated in reactions with H-acidic and multiple bond substrates, leading to further functionalized titanium complexes. Notably, **1b**, but not **1a**, could be reacted with an additional equivalent of carbodiimide, resulting in symmetric and asymmetric titanium bis(κ^1*N*-amidinato) complexes. This method of selective step-by-step reactions of bis(π–η^5:σ–η^1-pentafulvene)titanium complexes with carbodiimides and additional substrates was employed to synthesize functionalized titanium complexes. Ongoing research for the synthesis of complexes with a heteroallyl coordination mode to the titanium center is underway.

Author contributions

ME performed conceptualization, methodology, synthesis, characterization and writing of the manuscript. SB performed

synthesis and characterization. KS performed the computational work and writing of the computational part of the manuscript. MS performed the diffraction work. RB directed the work, acquired the funding and contributed to the final manuscript.

Data availability

All data for the experimental part and conclusions presented in this manuscript are included in the ESI.†

Conflicts of interest

There are no conflicts to declare.

Acknowledgements

Financial support by the DFG Research Training Group 2226 is kindly acknowledged.

References

1 (*a*) A. Williams and I. T. Ibrahim, *Chem. Rev.*, 1981, **81**, 589–636; (*b*) F. Kurzer and K. Douraghi-Zadeh, *Chem. Rev.*, 1967, **67**, 107–152.
2 J. C. Sheehan and K. R. Henery-Logan, *J. Am. Chem. Soc.*, 1959, **81**, 3089–3094.
3 Q. Shen, X. Ma, W. Li, W. Liu, Y. Ding, Z. Yang and H. W. Roesky, *Chem. – Eur. J.*, 2019, **25**, 11918–11923.
4 J. Koller and R. G. Bergman, *Organometallics*, 2010, **29**, 5946–5952.
5 (*a*) G. Veneziani, S. Shimada and M. Tanaka, *Organometallics*, 1998, **17**, 2926–2929; (*b*) H. Plenio and H. W. Roesky, *Z. Naturforsch., B:J. Chem. Sci.*, 1989, **44**, 94–95; (*c*) O. Lichtenberger, E. Pippel, J. Woltersdorf and R. Riedel, *Mater. Chem. Phys.*, 2003, **81**, 195–201.
6 (*a*) O. Meth-Cohn, D. Thorpe and H. J. Twitchett, *J. Chem. Soc. C*, 1970, 132–135; (*b*) B. Srinivas, C.-C. Chang, C.-H. Chen, M. Y. Chiang, I.-T. Chen, Y. Wang and G.-H. Lee, *J. Chem. Soc., Dalton Trans.*, 1997, 957–964; (*c*) W. J. Evans, J. R. Walensky, J. W. Ziller and A. L. Rheingold, *Organometallics*, 2009, **28**, 3350–3357; (*d*) C. N. Rowley, G. A. DiLabio and S. T. Barry, *Inorg. Chem.*, 2005, **44**, 1983–1991; (*e*) S. Schmidt, S. Gondzik, S. Schulz, D. Bläser and R. Boese, *Organometallics*, 2009, **28**(15), 4371–4376; (*f*) L. A. Koterwas, J. C. Fettinger and L. R. Sita, *Organometallics*, 1999, **18**(20), 4183–4190; (*g*) A. G. M. Barrett, M. R. Crimmin, M. S. Hill, P. B. Hitchcock, S. L. Lomas, M. F. Mahon and P. A. Procopiou, *Dalton Trans.*, 2010, **39**, 7393–7400; (*h*) C. Jones, *Coord. Chem. Rev.*, 2010, **254**, 1273–1289; (*i*) S. Gambarotta, S. Strologo, C. Floriani, A. Chiesi-Villa and C. Guastini, *Inorg. Chem.*, 1985, **24**, 654–660; (*j*) J. A. Tunge, C. J. Czerwinski, D. A. Gately and J. R. Norton, *Organometallics*, 2001, **20**(2), 254–260; (*k*) S. Li, J. Cheng, Y. Chen, M. Nishiura and Z. Hou, *Angew. Chem., Int. Ed.*, 2011, **50**, 6360–6363.
7 A. Goodwin and B. M. Novak, *Macromolecules*, 1994, **27**, 5520–5522.
8 (*a*) M. Haehnel, M. Ruhmann, O. Theilmann, S. Roy, T. Beweries, P. Arndt, A. Spannenberg, A. Villinger, E. D. Jemmis, A. Schulz and U. Rosenthal, *J. Am. Chem. Soc.*, 2012, **134**, 15979–15991; (*b*) E. P. Beaumier, C. P. Gordon, R. P. Harkins, M. E. McGreal, X. Wen, C. Copéret, J. D. Goodpaster and I. A. Tonks, *J. Am. Chem. Soc.*, 2020, **142**(17), 8006–8018.
9 X. Shi, S. Li, A. Spannenberg, F. Reiß and T. Beweries, *Inorg. Chem. Front.*, 2023, **10**, 3584–3594.
10 (*a*) A. W. Holland and R. G. Bergman, *J. Am. Chem. Soc.*, 2002, **124**(31), 9010–9011; (*b*) N. Hazari and P. Mountford, *Acc. Chem. Res.*, 2005, **38**(11), 839–849.
11 (*a*) K. Schwitalla, M. Claußen, M. Schmidtmann and R. Beckhaus, *New J. Chem.*, 2024, **48**, 18066–18074; (*b*) C. Adler, M. Diekmann, M. Schmidtmann and R. Beckhaus, *Z. Anorg. Allg. Chem.*, 2017, **643**, 732–735; (*c*) M. Manßen, N. Lauterbach, T. Wornescheck, M. Schmidtmann and R. Beckhaus, *Organometallics*, 2017, **36**(4), 867–876; (*d*) T. Oswald, T. Gelert, C. Lasar, M. Schmidtmann, T. Klüner and R. Beckhaus, *Angew. Chem.*, 2017, **129**, 12465–12469; (*e*) T. Oswald, T. Gelert, C. Lasar, M. Schmidtmann, T. Klüner and R. Beckhaus, *Angew. Chem., Int. Ed.*, 2017, **56**, 12297–12301; (*f*) T. Oswald, N. Lauterbach, M. Schmidtmann and R. Beckhaus, *Acta Crystallogr.*, 2018, **74**, 442–451; (*g*) M. Manßen, S. de Graaff, M.-F. Meyer, M. Schmidtmann and R. Beckhaus, *Organometallics*, 2018, **37**(23), 4506–4514; (*h*) S. de Graaff, A. Chandi, M. Schmidtmann and R. Beckhaus, *Organometallics*, 2021, **40**(19), 3298–3305; (*i*) M. Fischer, M. M. D. Roy, S. Hüller, M. Schmidtmann and R. Beckhaus, *Dalton Trans.*, 2022, **51**, 10690–10696; (*j*) S. de Graaff, K. Schwitalla, C. V. Haaker, N. Bengen, M. Schmidtmann and R. Beckhaus, *Dalton Trans.*, 2022, **51**, 12502–12511; (*k*) S. de Graaff, M. Eilers, J. Buschermöhle, N. Bengen, A. Dierks, M. Schmidtmann, M. Manßen and R. Beckhaus, *Eur. J. Inorg. Chem.*, 2023, **26**, e202200637; (*l*) S. de Graaff, K. Schwitalla, H. Thye, Z. Yusufzadeh, M. Willms, M. Schmidtmann and R. Beckhaus, *Chem. – Eur. J.*, 2023, **29**, e202203846.
12 (*a*) M. Manßen, I. Weimer, C. Adler, M. Fischer, M. Schmidtmann and R. Beckhaus, *Eur. J. Inorg. Chem.*, 2018, 131–136; (*b*) M. Manßen, A. Dierks, S. de Graaff, M. Schmidtmann and R. Beckhaus, *Angew. Chem., Int. Ed.*, 2018, **57**, 12062–12066.
13 M. Eilers, K. Schwitalla, T. Dirksen, M. Schmidtmann, M. Fischer and R. Beckhaus, *Organometallics*, 2023, **42**(11), 1043–1047.
14 M. Manßen, C. Adler and R. Beckhaus, *Chem. – Eur. J.*, 2016, **22**, 4405–4407.
15 N. J. Hill, J. A. Moore, M. Findlater and A. H. Cowley, *Chem. Commun.*, 2005, 5462–5464.

16 F. Montilla, D. del Río, A. Pastor and A. Galindo, *Organometallics*, 2006, **25**, 4996–5002.
17 L.-J. Wu, Q. Wang, J. Guo, J. Wei, P. Chen and Z. Xi, *Angew. Chem., Int. Ed.*, 2023, e202219298.
18 P. Pyykkö and M. Atsumi, *Chem. – Eur. J.*, 2009, **15**, 186–197.
19 M. Diekmann, G. Bockstiegel, A. Lützen, M. Friedemann, W. Saak, D. Haase and R. Beckhaus, *Organometallics*, 2006, **25**(2), 339–348.
20 F. H. Allen, O. Kennard and D. G. Watson, *J. Chem. Soc., Perkin Trans. 2*, 1987, **3**, 1–19.